Restoration of T cell Effector Function, Depletion of Tregs, and Direct Killing of Tumor Cells: The Multiple Mechanisms of Action of a-TIGIT Antagonist Antibodies

Authors and affiliations

J. Preillon[1*], J. Cuende[1*], V. Rabolli[1*], L. Garnero[1], M. Mercier[1], N. Wald[1], A. Pappalardo[3], S. Denies[1], D. Jamart[1], A. Michaux[1], R. Pirson[1], V. Pitard[3], M. Bagot[5], S. Prasad[1], E. Houthuys[1], M. Brouwer[1], R. Marillier[1], F. Lambolez[1], J.R. Marchante[1], F. Nyawouame[1], M.J. Carter[2], V. Bodo[1], A. Marie-Cardine[5], M.S. Cragg[2], J. Dechanet-Merville[3,4], G. Driessens[1*], C. Hoofd[1*]

[*]Authors equally contributed to the work

[1]iTeos Therapeutics, Gosselies Belgium and Cambridge USA.

[2]Antibody & Vaccine Group, Centre for Cancer Immunology, Cancer Sciences Unit, Southampton University Faculty of Medicine, Southampton, UK

[3]ImmunoConcEpT, UMR 5164, Bordeaux University, CNRS, Bordeaux, France

[4]Team labeled LIGUE 2017

[5]INSERM U976, Université de Paris, Hôpital Saint Louis, Paris, France

Running title (no more than 60 characters)

Multiple Mechanisms of Action of anti-TIGIT Antagonists

Keywords (5 keywords)

anti-TIGIT Antagonists, Regulatory T cells, ADCC, gamma/delta T cells, Immune checkpoint inhibitor

Financial support (source and number of grants, for each author)

Authors indicated with [1] are full-time employee of iTeos Therapeutics. Authors with [2, 3, 4] received funding from iTeos Therapeutics for activities linked to this manuscript.

Corresponding author

Gregory Driessens
Rue des Frères Wright, 29
6041 Gosselies, Belgium
Phone: 0032 (0)71 919962
Email: gregory.driessens@iteostherapeutics.com

Conflict of interest disclosure statement

See: **Conflict of Interest Policy**

Abstract

TIGIT is an immune checkpoint inhibitor expressed by effector $CD4^+$ and $CD8^+$ T, NK cells and regulatory T-cells. Inhibition of TIGIT-ligand binding using antagonistic anti-TIGIT monoclonal antibodies (mAbs) has shown *in vitro* potential to restore T-cell functions and therapeutic efficacy in murine tumor models when combined with an anti-PD(L)-1 antibody. Here, we demonstrate for the first time, broader TIGIT expression than previously reported in healthy donors and cancer patients: being observed on γδ T-cells, particularly in CMV-seropositive donors and on tumor cells from hematological malignancies such as cutaneous T -cell lymphoma. Quantification of TIGIT density revealed tumor-infiltrating Treg as the population expressing the highest receptor density. Consequently, the therapeutic potential of anti-TIGIT mAbs might be broader than the previously described anti-PD(L)-1 like restoration of αβ T-cell function. In addition to αβ T-cell re-invigoration, CD155 also mediated inhibition in γδ T-cells, an immune population not previously described to be sensitive to TIGIT inhibition, and could be fully prevented via use of an antagonistic anti-TIGIT mAb (EOS884448). In PBMC from cancer patients, as well as TILs from mice, the higher TIGIT expression in Treg correlated with strong antibody-dependent killing and preferential depletion of this highly immunosuppressive population. Accordingly, ADCC-enabling anti-TIGIT mAb had superior antitumor activity, that was depending on Fcγ receptor engagement. In addition, we induced direct killing of TIGIT-expressing tumor cells both in human patient material and animal models, demonstrating strong rational for therapeutic intervention in heme malignancies. These findings reveal broad therapeutic opportunities for anti-TIGIT mAbs in cancer therapeutics.

Introduction

T cell immunoglobulin and immunoreceptor tyrosine-based inhibitor motif (ITIM) domain (TIGIT) is a member of the poliovirus receptor (PVR)/nectin family and shares structural similarity with other immunoglobulin superfamily receptors. TIGIT contains a type 1 transmembrane domain and an intracellular domain with an immunoreceptor tyrosine-based inhibitory motif (ITIM) (1). Cell-surface expression of TIGIT is mainly restricted to lymphocytes including effector $CD4^+$ and $CD8^+$ T and natural killer (NK) cells (2,3). TIGIT is also constitutively expressed by regulatory T cells (Treg), where it is involved in regulating cellular homeostasis and function of this immunosuppressive T cell subset (2).

TIGIT is bound by several ligands of the PVR/nectin family with the highest affinity for CD155 (PVR) followed by CD112 (Nectin-2 or PVRL2) and CD113 (Nectin-3 or PVRL3) (1). CD96 and CD112R (PVRIG) represent additional inhibitory receptors of the same family which share common ligands and negatively modulate the effector functions of NK and T cells. CD226 (DNAM-1), in contrast, functions as a co-stimulatory receptor and shares CD155 and CD112 ligands with TIGIT. TIGIT expression has been observed to be upregulated in cancer patients, with higher expression on tumor-infiltrating lymphocytes (TILs) compared with circulating peripheral blood mononuclear cells (PBMCs) or immune cells from tumor-adjacent tissue in patients with liver cancer (4). Similarly, a higher proportion of $TIGIT^+$ $CD4^+$ T cells was observed in skin and PBMCs from cutaneous T cell lymphoma (CTCL) patients than healthy donors (5). $TIGIT^+$ T cells have impaired effector function relative to their $TIGIT^-$ counterparts (6). Conversely, $TIGIT^+$ Treg cells are more effective at suppressing effector T cell activation than their $TIGIT^-$ counterparts (7,8) and inhibit Th1 and Th17 responses through a mechanism dependent on fibrinogen-like protein 2 (2).

The function of TIGIT and CD226 is analogous to that of cytotoxic T lymphocyte-associated antigen-4 (CTLA-4) and CD28. CD226 is expressed on naïve T cells, while TIGIT expression is upregulated upon activation or inflammatory stimuli (3,9,10). TIGIT elicits immune suppression through several mechanisms: 1) direct ITIM-mediated negative signaling; 2) competition between TIGIT and CD226 for ligand-binding that display higher affinities for TIGIT; 3) enhanced IL-10 and reduced IL-12 production by dendritic cells (DC) after ligation of TIGIT on CD155 expressed at their surface leading to a tolerogenic DC phenotype; and 4) direct disruption of costimulatory signaling mediated by CD226 due to heterodimerization of TIGIT with CD226 (1,3,11,12).

Because TIGIT ligands are highly expressed on tumor cells in a wide array of cancers (13), interaction with $TIGIT^+$ TILs is a common mechanism to create an immunosuppressive tumor microenvironment (TME) for infiltrating T and NK cells. Consequently, TIGIT is a relevant target of interest for cancer immunotherapy (14), as supported by preclinical studies. Pharmacological blockade of TIGIT with antagonistic antibody inhibits tumor growth in murine tumor models either alone or in combination with immune checkpoint inhibitors, e.g. anti-PD1 or anti-PDL1 antibodies (3,15–19). The degree of antitumor response depends upon the isotype of the antagonistic anti-TIGIT monoclonal antibody (anti-TIGIT mAb) and whether it engages CD226, as efficacy is lost if CD226 is simultaneously blocked (3). Furthermore, *ex-vivo* antigen specific re-stimulation of T cells from vaccinated cancer patients demonstrated the ability of anti-TIGIT mAb alone or in combination with anti-PD1 to increase the effector functions of T cells targeting tumor antigens (20). Based on these findings, several anti-TIGIT Abs in various forms, e.g. IgG1, IgG1 variant with low affinity to Fcγ receptors (FcγR), and IgG4 are being clinically evaluated (21).

These observations led us to investigate the potential for therapeutic intervention with anti-TIGIT mAb, and we showed, for the first time, that in addition to the well-described PD(L)-1 like activity to restore αβ T cell function, anti-TIGIT mAb therapy increases the function of γδ T cells isolated from healthy donors and also mediate direct killing of tumor cells and immunosuppressive Treg both in cancer patient samples and preclinical mouse models. This latter activity was dependent upon the affinity to activatory FcγR. These findings reveal novel immunosuppressive mechanisms of TIGIT in cancer and broader therapeutic opportunities for anti-TIGIT drugs and support the selection of anti-TIGIT mAbs with high affinity for activatory FcγR as the pharmacophore with the greatest therapeutic potential for cancer patients.

Material and Methods

Tumor microarray and fresh tumor dissociation

A total of twenty-one formalin-fixed paraffin-embedded (FFPE) disease-specific tissue microarrays (TMAs) blocks were assembled at Institut de Pathologie et de Génétique (IPG, Gosselies, Belgium). The TMAs contained 55-60 cores derived from nine cancer types, with 13-51 donors per cancer type (Table 2). Sections of 4-5 μm thickness were cut at IPG. The research project was approved by Jules Bordet Ethical Committee (Brussels, Belgium, #CE2797).
Tumors surgically removed after informed consent were collected by BioPartners. Resections were placed directly in cold AQIX RS-I media for transport and, immediately after arrival (within 28 hours after surgery), minced with scalpels and dissociated using the Tumor Dissociation Kit and the GentleMax Dissociator (Miltenyi Biotec). Single cell suspensions were obtained by pooling three successive dissociation rounds and filtering through a 70 μm nylon mesh cell strainer.

PBMC and T cell isolation

Blood samples associated with tumor samples from cancer patients, taken after informed consent were provided by BioPartners. Venous blood from healthy volunteers (approved by the Ethics Committee, FOR-UIC-BV-050-01-01 ICF_HBS_HD Version 7.1), was obtained from Tivoli Hospital, La Louvière, Belgium. PBMCs were isolated by lymphoprep density gradient centrifugation used in combination with SepMate™ (Stemcell Technologies) tubes according to the manufacturer's instructions. After purification, cells were immediately characterized by flow cytometry or frozen in 90% FBS, 10% DMSO in liquid nitrogen. $CD8^+$ T cells were purified from frozen human PBMCs according to manufacturer's recommendations using negative selection (Stemcell Technologies).

Flow cytometry

$2x10^5$ (for antibody mix) or 3.10^4 cells (for single stain controls) were distributed in 96 well U-bottom plates and stained per manufacturer's instruction using filtered PBS, 2mM EDTA, 0.1% BSA FACS buffer, and Brilliant Stain buffer (BD Biosciences). Cells were blocked with Human FcBlock for 10 min at room temperature (RT) before incubation for 20 min with antibody cocktail at 4°C. To quantitate TIGIT receptor cell surface expression, Quantibrite™ beads (BD Biosciences) were resuspended following manufacturer's instructions and processed identically to other samples. Cells were washed twice and fixed using BD Cell Fix buffer prior to acquisition. Viable single cells were gated on Forward and Side scatter or using fixable viability dye (FVD) efluor520.
For *ex-vivo* stimulated samples, 2.10^5 PBMCs per condition were suspended in X-vivo15 medium (Westburg) and activated as previously described (22).
Cell samples were analyzed using a 4-laser LSR Fortessa flow cytometer (BD Biosciences) using Diva software and analyzed with FlowJo software v10.6.1 (FlowJo, LLC).
Antibodies and panels used for flow cytometry analysis are listed in **supplementary Table 1**.

CD155 staining by IHC

CD155 and pancytokeratins were stained according to methods described in supplementary material.

Co-culture of CD155-expressing cells and $CD8^+$ T cells

CD155 APC/CHO-K1 (Promega) cells were seeded in U-bottom 96-well plates according to manufacturer's recommendations and incubated at 37°C, 5% CO_2 overnight. Then, 10^5 healthy donor $CD8^+$ T cells were subjected to increasing concentrations of anti-TIGIT Ab EOS884448 (final concentrations 0.011nM to 333nM/75µL of full medium) and were added to CD155 aAPC/CHO-K1 cells and incubated at 37°C, 5% CO_2 for 5 days. IFNγ concentrations were assessed in cell supernatants by ELISA (Affymetrix eBioscience).

In vitro ADCC assays of human PBMCs

Cryopreserved isolated PBMCs from healthy volunteers and cancer patients were provided by ImmunXperts (Gosselies, Belgium), and ConversantBio (Huntsville, Alabama). PBMCs were thawed and resuspended in complete RPMI medium supplemented with 10% FBS + 50U/mL Pen/Strep (Westburg). $2.5x10^5$ cells were distributed per well and incubated at 37°C, 5% CO_2 for 20 h with either anti-TIGIT mAb, its corresponding IgG isotype control (BioXcell), or Rituximab at a final concentration of 6.6 nM. Cells were then stained for surface markers as indicated in **Supplementary Table 1**. After washing, cells were fixed and, immediately before acquisition, AccuCheck Counting beads were added for absolute quantification following manufacturer's specifications. Data were acquired as described for flow cytometry. The absolute number of cells per µL was calculated for different T and B cell populations after exclusion of FVD^+ cells. The % of specific lysis was calculated as being equal to (1- (absolute number of cells per µl in corresponding Ab treated conditions / average absolute number of cells per µL of the triplicates of the isotype control Ab conditions)) x 100.

γδ T cell functional assay

PBMCs from CMV^+ donors were isolated by gradient centrifugation, resuspended in complete RPMI supplemented with 10 % FCS at a density of 10^5 cells/mL, and seeded in round-bottomed 96-well plates. PBMC were isolated from blood donor from blood bank (Etablissement Français du Sang Aquitaine Limousin). Cells were cultured with IL-15 (20 ng/mL) and Vδ1 γδ T cells T cells were activated with 10 µg/mL anti-Vδ1 antibody (clone R9.12, Beckman Coulter). Recombinant human CD155-Fc (R&D Systems) was added at 10 µg/mL, with or without 66.6ηM EOS884448. Cells were cultured for 48h at 37 °C, 5% CO_2, supernatant was then collected, and IFN-γ concentration measured by ELISA (MabTech kit). Production of Granzyme B, GM-CSF, and TNFα was assessed by Cytometric Bead Array (Flex Set CBA, BD Biosciences) as per the manufacturer's recommendations.

Mice

Eight week-old female BALB/c mice (Charles River Laboratories) were housed at the specific pathogen free (SPF) facility of the IMI, Gosselies, Belgium in individually ventilated cages (IVCs). All experiments were performed in accordance with national and institutional guidelines for animal care and the approval of the local Animal Ethics Committee. For experiments conducted in Southampton, 8- to 12-week-old female BALB/c and Fc receptor gamma chain knock-out (FcR γ chain KO) generated as previously described (23) mice were housed in individually ventilated cages (IVCs). Animal experiments were conducted according to the UK Home Office license guidelines and approved by the University of Southampton Ethics Committee. During the study, the care and use of animals were in accordance with the regulations of the Association for Assessment and Accreditation of Laboratory Animal Care.

Culture of murine cell lines

The CT26 (ATCC® CRL-2638™), Hepa1-6, and EL4 (ATCC® TIB-39™) tumor cells were maintained *in vitro* as a monolayer culture in RPMI (CT26) or DMEM (Hepa1-6 and EL4) medium supplemented with 10% FBS and 1% HEPES buffer at 37ºC, 5% CO_2. Cells in exponential growth phase were harvested and quantitated by cell counter before tumor inoculation. EL4 lymphoma cells were transduced at GIGA Institute (U.Liège) with pLV EF1A mTigit-IRES-EmGFP vector to stably express mouse TIGIT (EL4-mTIGIT) or control vector pLV EF1A-EmGFP encoding GFP alone (EL4-GFP). Transduced EL4 were cloned and grown in medium with 13.33 μg/mL of Blasticidin (ThermoFisher Scientific).

Tumor growth and treatments

CT26 ($5x10^5$), EL4-mTIGIT ($1x10^6$), EL4-GFP ($0.2x10^6$), Hepa1-6 ($5x10^6$) tumor cells were inoculated subcutaneously in the right flank of BALB/c, C57BL/6 (both strains from Charles River Laboratory), or activatory FcR γ chain KO mice (23).Mice were randomized and treated using PBS, mIgG2a isotype (200 μg/mouse, BioXCell BE0085), anti-TIGIT mIgG2a (20 or 200 μg/mouse), anti-TIGIT mIgG1 (200 μg/mouse), anti-TIGIT hIgG1 (200 μg/mouse), anti-TIGIT hIgG1-N297A (200 μg/mouse) (all a-TIGIT for mouse models were produced at UProtein, The Netherlands), anti-PD-1 (200 μg/mouse, BioXCell BE0146), anti-4-1BB (5 μg/mouse, BioXCell BE0239), anti-OX-40 (20 μg/mouse, BioXCell BE0031), or anti-GITR (10 μg/mouse, BioXCell BE0063), as indicated for specific models, and measured as previously described (22). Because human a-TIGIT mAb EOS884448 does not cross-react with mouse TIGIT, the anti-TIGIT antibody used in murine models is a surrogate antibody, EOS931296. Some antibodies were combined, as indicated in the figure legends. All antibodies were administered by intraperitoneally injection every 3 days for a total of 3 to 4 injections. Rechallenge experiments were performed on mice that experienced complete regression. CT26 tumor cells were inoculated as described above on day 70 after the first tumor inoculation. EMT6 cells were inoculated in the intramammary gland at day 90 after the first CT26 inoculation at the dose of 0.1×10^6 cells/mouse. A cohort of naïve mice was inoculated in parallel to confirm tumor cell viability and ability to grow.

Flow cytometry on dissociated CT26 murine tumors

Two days after the second antibody treatment and 10 days post-tumor inoculation, CT26 tumor bearing mice were sacrificed and eight tumors per group were collected in ice-cold PBS and prepared for flow cytometric analysis. Surface staining was performed according to **Table 1**. Cells were fixed overnight at 4°C, treated again with Fc block (anti-CD16/CD32, eBioscience) for 15 min at RT, followed by intracellular staining with FoxP3-APC (supp Table 1) in permeabilization buffer for 30 min at 4°C. Cells were washed and resuspended in FACS buffer prior to acquisition. For *ex vivo* stimulation, cells were treated as previously described (22) and according to **supplementary Table 1**. Data were acquired on a MacsQuant flow cytometer (Miltenyi Biotech) and analyzed with FlowJo™ V10.1

Measurement of TIGIT expression and *ex-vivo* ADCC assay in blood samples from Sézary syndrome patients

The study was approved by institutional ethic comittee (Saint Louis Hospital, Paris, France) and blood was obtained from Sézary patients after written informed consent. To distinguish between Sézary patients' tumor and normal $CD4^+$ T cells, predetermination of the malignant clone TCR-Vβ rearrangement was performed on peripheral blood (Beckman Coulter TCR-Vβ repertoire kit, IM3497).

Only patients whose malignant clone could be identified through its TCR- Vβ rearrangement were processed for evaluation of TIGIT expression profile on immune cells. TIGIT expression was monitored in normal and malignant $CD4^+$ T, $CD8^+$ T, B, and NK cells by flow cytometry using antibodies described in **supplementary Table 1**.
For ADCC assay, patient samples were treated as described previously (24). Purified $CD4^+$ T cells were pre-incubated for 30 min at RT with an hIgG1, anti-TIGIT Ab (EOS884448), or positive control antibody corresponding to Alemtuzumab sequence (produced at UProtein, The Netherlands) at 66.6ηM and then mixed with the autologous sorted NK lymphocytes at the indicated E:T ratios. Incubation was conducted for 4h 30min at 37°C, 5% CO_2.

Statistical Analyses

Statistical analyses are described in the figure legends. For tumor growth curves, data were fitted with a linear mixed model using SAS JMP® version 13 after log transformation of tumor volumes. Fixed effects included time and treatment. Polynomial functions of time were included based on significance of the polynomial term in sequential tests. The necessity to include random effects was assessed by a Wald test. Good model fit was assessed by plotting the fitted versus observed tumor growth curves and by residual analysis. A treatment difference in tumor growth was tested by a joint hypothesis test for the interaction terms of time and treatment (25).

Results

Expression of TIGIT and CD155 in healthy volunteers and cancer patients

Expression of TIGIT and CD155 was tested in PBMCs from both healthy donors and cancer patients with multiple solid tumor indications. TMA analysis of CD155 by IHC (**Supp Fig. 1A**) showed a high expression, especially in pancreas, prostate, and kidney cancers, which all had a median value greater than 20% $CD155^{high}$ tumor cells (**Fig. 1A**). To characterize TIGIT expression in different immune populations and explore its modulation in the tumor-environment, we compared the proportion of TIGIT-expressing cells as well as number of TIGIT molecules per cell in PBMCs from healthy donors or matched PBMCs and TILs from cancer patients. We noticed an increase in the proportion of TIGIT-expressing cells in the NK and T cell populations analyzed ($CD4^+$, $CD8^+$, Treg, NK, and NKT cells) in PBMCs from cancer patients versus those from healthy donors TIGIT expression on TILs was further enhanced, particularly in $CD4^+$, $CD8^+$, Treg and NKT cell populations, but not on NK cells. Treg and $CD8^+$ T cells showed the highest frequency with more than 85% $TIGIT^+$ cells (**Fig. 1B**). Interestingly, the number of TIGIT receptors per cell was also higher on PBMCs from cancer patients than healthy donors in all tested immune populations. While the number of receptors observed between PBMCs and TILs was similar for most populations, it appeared that there was a 2-fold increase of TIGIT on Treg cells in the tumor. As expected, non-immune populations (non-T/NK cells) had a very level level of expression of TIGIT (**Fig 1C**). Overall, TIGIT and its ligand CD155 were highly expressed in tumors with an increased proportion of TIGIT-expressing cells in TILs and the highest level of TIGIT in regulatory T cells.

TIGIT-expressing TILs have impaired functionality, reversed by anti-TIGIT mAb

To characterize and compare the functional activity of T cells expressing or lacking TIGIT, we measured cytokine production after *ex vivo* stimulation of human TILs. In both $CD4^+$ and $CD8^+$ T cell populations, the proportion of IFNγ-, IL-2-, or TNFα-expressing cells was much higher in $TIGIT^-$ cells versus $TIGIT^+$ cells. This confirms the exhausted phenotype of TIGIT-expressing TILs (**Fig. 2A**). Interestingly, this exhausted phenotype was more pronounced in TILs than PBMCs; $TIGIT^+$ cells in PBMCs maintained the ability to produce TNFα or IFNγ after stimulation (**Fig. 2B**).
To test the potential of anti-TIGIT mAb EOS884448 to restore functional activity of $TIGIT^+$ cells, we first confirmed its ability to prevent CD155 binding and increase the functional activity of Jurkat cells engineered to overexpress TIGIT as measured with a reporter assay (**Supp Fig. 2**). Then, we tested the effect of anti-TIGIT mAb on $CD8^+$ T cells from healthy donor PBMCs activated in the presence of CD155-expressing cells and demonstrated that blocking TIGIT restored secretion of IFNγ (**Fig. 2C**). These results showed that $TIGIT^+$ T cells from cancer patients have an exhausted phenotype and that anti-TIGIT Abs have the potential to improve the function of immune cells in the periphery and in the TIGIT-rich TME.

CD155/TIGIT axis is immunosuppressive in γδ T cells and can be reverted by EOS884448

Engagement of TIGIT also has an immunosuppressive effect on γδ T cells, which can be prevented with an anti-TIGIT mAb. Immunosuppressive activity of TIGIT has been well described for αβ T cells, but nothing is known regarding its inhibitory function on non-conventional γδ T cells. We observed a high expression of TIGIT on γδ T cells, even higher

than on NK or αβ T cells. γδ T cells can be divided into two populations according to expression of the Vδ2 chain of the TCR, which distinguishes the phosphoantigen-responding $V\delta2^+$ γδ T cells and the CMV-responding $V\delta2^-$ γδ T cells (26). **Figure 3A** shows that the percentages of $TIGIT^+$ cells and the intensity of TIGIT expression were higher among $V\delta2^-$ than $V\delta2^+$ γδ T cells. Of interest, $V\delta2^-$ γδ T cells from CMV-seropositive donors exhibited higher TIGIT expression than CMV-seronegative ones (**Fig. 3A**). Increased expression of TIGIT in CMV-seropositive donors was also seen for αβ T cells, while no difference was observed for NK cells or $V\delta2^+$ T cells. CMV-seropositivity did not uniformly affect all inhibitory checkpoints, since CMV serostatus had no influence on PD1 expression on γδ T cells, while NK and αβ T cells had higher proportions of $TIGIT^+$ cells in CMV seropositive samples (**Fig 3B**). As previously observed for αβ T cells, the $TIGIT^+$ $V\delta2^-$ γδ T cells comprise mainly differentiated cells with cytotoxic potential as characterized by their $CD45RA^+$ $CD27^-$ $CD28^-$ $granzyme^+$ phenotype (**Supp Fig 3**). We next determined if TIGIT expression could elicit an immunosuppressive signaling in γδ T cells, and if anti-TIGIT treatment could functionally restore activity of γδ T cells as observed in αβ T cells (**Fig. 2**). We activated Vδ1 T cells within PBMC from CMV^+ donors with an agonist anti-Vδ1 mAb in the presence of a soluble form of CD155 with and without anti-TIGIT mAb EOS884448. CD155 elicited a strong inhibitory effect on Vδ1 T cell activation as measured by a decrease of IFNγ secretion. The addition of a-TIGIT mAb fully prevented CD155-mediated inhibition (**Fig. 3C**). This inhibitory effect induced by CD155 and prevented by EOS884448 was not restricted to IFNγ and was also observed with other pro-inflammatory cytokines (**Fig 3D**). In conclusion, TIGIT is be strongly expressed in γδ T cells - particularly in CMV-seropositive individuals who represent about half of the population in western countries, and the inhibitory function of TIGIT on these cells can be prevented by the anti-TIGIT EOS884448 mAb.

Anti-TIGIT Ab EOS884448 mediates preferred direct cytotoxicity of Treg

Since Treg population shows a higher proportion of $TIGIT^+$ cells and higher number of TIGIT receptors per cell than other immune populations (**Fig. 1C**), we measured the ability of anti-TIGIT Ab to induce direct killing of Treg through ADCC as a second mechanism of action, independent of the prevention of ligand binding. To validate direct cytotoxic potential, we compared several isotypes of anti-TIGIT Ab (human IgG1, IgG2 and IgG4) and confirmed, that only hIgG1 mAb could engage FcγR on effector cells and induce direct ADCC (**supplementary Fig. 4**). We then tested the cytotoxic potential in PBMCs from a cancer patient. There was a clear lytic potential of EOS884448 on Tregs, while $CD45RO^+$ memory $CD4^+$ or $CD8^+$ T cells that express the next highest level of TIGIT in non-Treg cells were not impacted (**Fig 4A**). Similar assays were performed on samples from seven patients with four different types of solid tumors and confirmed the cytotoxic potential against Treg population. Except for one sample from a bladder cancer patient that demonstrated high cytotoxicity in all populations, there was a significant difference with stronger ADCC activity against Treg populations than in memory T cells (**Fig 4B**). This increased cytotoxic potential in Treg correlated with a higher expression of TIGIT receptors per cell and could explain the difference in cytotoxic potential observed in various immune populations (**Fig. 4C**).

TIGIT inhibition shows strong antitumor therapeutic effects that depends on mAb isotype and binding to FcγR

Preclinical models using anti-TIGIT mAbs have shown different outcomes; one study showed no single agent efficacy against CT26 tumors (3), while another demonstrated a

potent response (15). To better characterize the potency of a mouse surrogate anti-TIGIT mAb, we conducted similar experiments in tumor models such as CT26 and Hepa1-6 and demonstrated strong tumor growth delay with some complete response in both models when anti-TIGIT mAb was built on the mouse IgG2a isotype that effectively engages activatory Fcγ receptors (FcγR) (**Fig 5A**). In contrast, when the same anti-TIGIT Ab clone was built on a mouse IgG1 isotype, which engages less strongly with activatory FcγR, the antitumor activity was completely lost (**Fig 5B**). To understand if the antitumor effect of anti-TIGIT mAb was dependent on engagement of activatory FcγR, we tested the activity of mIgG2a anti-TIGIT mIgG2a mAb FcRγ chain KO mice, which lack surface expression and signaling of all activatory FcγR. Similarly to mIgG1 in wild-type animals, anti-TIGIT mIgG2a had no activity in FcR γ chain KO mice (**Fig 5C**). To further support the importance of FcγR engagement and provide insight into the mechanism of anti-TIGIT Ab therapy, we assessed effects on TILs and observed an association between the specific antitumor efficacy of anti-TIGIT mIgG2a mAb with partial depletion of Treg population within the TME (whereas $CD8^+$ T cells were not impacted) (**Fig 5D**) and an increase of $IFN\gamma^+$-producing $CD4^+$ and $CD8^+$ T cells within the TME (**Fig 5E**). Finally, anti-TIGIT mAb had been described to act synergistically with anti-PD1 (3). To further test the combination potential of anti-TIGIT mAb, we combined treatment of anti-TIGIT mAb with Abs targeting co-stimulatory molecules (4-1BB, OX-40, or GITR) and experienced strong additive or synergistic effect of the combination treatment that was not limited to PD1 (**Fig 5F**). Importantly, all mice that experienced complete response against CT26 developed a long-lasting tumor specific memory responses capable of protecting them against re-challenge with CT26, but not EMT6, tumor cells (**Supp Fig 5**).

TIGIT is expressed by specific cancer cells and represents a target for direct cytotoxicity

TIGIT has been described to be specifically expressed in immune cells (1). Following investigation of public databases for TIGIT gene expression in cancers, we identified a high proportion of heme malignancies among samples with high expression level (**Supp Fig. 6)**. To determine if this observation was due to strong TIGIT expression by immune cells in these blood cancers or to expression on tumor cells themselves, we acquired fresh samples from patients with Sezary syndrome (SS), a particular form of cutaneous T cell lymphoma (CTCL) with circulating clonal $CD4^+$ tumor cells. To differentiate the normal and tumor $CD4^+$ T cell population in these samples, we first determined the TCR-Vβ rearrangement corresponding to the tumor clone. TIGIT was stained on both $CD4^+$ populations, and the results clearly showed the existence of a $TIGIT^+$ population on the $CD4^+$ tumor cells (**Fig 6A**). When data from 23 patients were pooled, more than 80% of tumor cells in 21 of 23 patients expressed TIGIT. This confirmed, for the first time, a high level of TIGIT expression on tumor cells themselves (**Fig 6B**). Normal $CD4^+$ T cells had moderate expression as observed in other tumors (**Fig 1**).

Since TIGIT was found on the surface of tumor cells, we explored the possibility for anti-TIGIT mAb EOS884448 to have a direct anti-tumor cytotoxic effect. Fresh blood samples of SS patients were tested for ADCC potential against different TIGIT-expressing populations using autologous NK effector cells. Direct cytotoxicity was observed on tumor $CD4^+$ cells in 3 out of 4 patient samples, that increased with the effector:target (E:T) ratio. This was either undetectable or significantly reduced in non-malignant $CD4^+$ or NK cells subsets (**Fig. 6C**). To further confirm that anti-TIGIT mAb could demonstrate potential antitumor effects through direct cytotoxicity on tumor cells, we established a mouse model with EL4 T cell

lymphoma engineered to express mouse TIGIT. Similar to results observed in human cancer samples, mouse surrogate anti-TIGIT mAb could lyse EL4-mTIGIT cells *in vitro* (**Supp Fig 7**). We then tested the *in vivo* potential of anti-TIGIT mAb therapy against established EL4 tumors and showed, that anti-TIGIT mAb therapy is only active in EL4-expressing TIGIT but not in control EL4 cells just expressing GFP (**Fig 6D**). Finally, the single amino acid mutation N297A in anti-TIGIT mAb that prevents binding to FcγR totally abolishes its therapeutic potential and confirms the FcγR-mediated mechanism of action in this setting (**Fig 6D**). Altogether, these results show, for the first time, the direct anticancer potential of an anti-TIGIT mAb therapy to not only by preventing immunosuppression through TIGIT blockade and elicit depletion of Treg cells but also evoke a third mechanism of action linked to its direct cytotoxicity of TIGIT-expressing tumor cells.

Discussion

Cancer immunotherapy with immune checkpoint inhibitors (ICIs) has demonstrated long-term responses in some cancer patients (27). Three ICI drugs have been approved (CTLA-4, PD-1, and PD-L1) in multiple indications, but durable responses are still limited to a minority of patients, and drug resistance and/or toxicity is frequent (28). This highlights the need for the development of new drugs that manipulate additional ICI targets and for combination strategies. Several anti-TIGIT mAbs are currently under clinical evaluation as single agents or in combination with anti-PD(L)1 mAb, but few results from phase 1 trials have been released to date (21).

While it was anticipated that, similar to the anti-PD(L)1 mAb effect, the main activity of anti-TIGIT mAbs would be the reactivation of exhausted αβ T cells, during the course of the preclinical development of EOS884448, a novel human IgG1 anti-TIGIT mAb, we discovered several additional potential mechanisms of action. First, we demonstrated that TIGIT expression was not restricted to αβ T cells but was also observed at high levels on non-conventional γδ T cells. Since γδ T cells have been identified as the most favorable cancer-wide prognostic signature for outcome and to play an antitumor roles (29,30), we explored the possible mechanistic function of TIGIT on that immune cell population. Similar to αβ T cells, we confirmed that γδ T cells express TIGIT and are sensitive to CD155-mediated immunosuppression. The addition of anti-TIGIT mAb EOS884448 could fully restore the secretion of pro-inflammatory cytokines, demonstrating its ability to prevent TIGIT ligand-mediated immunosuppression of γδ T cells in TME-like conditions. While previous reports had indicated the low expression and limited mechanistic function of PD1 and TIGIT in the Vδ2 subpopulation of γδ T cells (31,32), our data suggest that other γδ T cell subpopulations, such as Vδ1 cells, express TIGIT and are sensitive to TIGIT-mediated immunosuppression, which can be prevented by antagonist molecules. While such activity had been observed in αβ T cells and NK cells, to our knowledge, this is the first demonstration that TIGIT can mediate suppressive activity on γδ T cells and could be involved in TME-induced suppression known to induce deficient γδ T cell functionality or polarization toward Treg phenotype (32,33). To further confirm the relevance of our finding in disease setting, additional work will be needed to specifically examine the effect of TIGIT on γδ T cells in the context of animal tumor models.

Similar to a previous report that showed increased TIGIT expression in the TME (3,4,13), we observed, for different T cell populations, a higher proportion of $TIGIT^+$ cells in TME as compared to PBMCs from cancer patients and healthy volunteers. Further, the proportion of tumor-infiltrating (TI) $TIGIT^+$ Treg was close to 100%, which is in agreement with data comparing the expression of different immune checkpoints in Treg (34). Comparing the density of TIGIT molecules, we noticed that the highest expression was on TI-Tregs while the level of TIGIT receptors on $CD8^+$ T cells present in the TME was similar or lower than on PBMCs from matched cancer patients. Treg in the TME, and particularly $TIGIT^+$ Treg that form a distinct Treg subset, are known to play a strong immunosuppressive role and are associated with poor outcome in several cancer indications (2,35). Our observation suggested the potential of anti-TIGIT mAbs to mediate preferential deletion of the $TIGIT^+$ Treg population over other $TIGIT^+$ T cell populations. Preferential Treg depletion could be linked to higher expression levels (**Fig. 1 and 4C**) or to a different cell intrinsic mechanism that renders them susceptible to ADCC-mediated lysis, since other mAbs targeting GITR, CTLA4 or 4-1BB have also been reported to preferably deplete Treg cells (36,37, 38). Since this hypothesis that had not yet been described for anti-TIGIT mAb, we compared depletion

mediated by ADCC-enabled molecules in cancer patients' PBMCs samples and confirmed greater Treg depletion than in other T cell populations also present in the TME. Due to limitations in sample access, we could not assess TIL material in which TIGIT expression in Treg is further increased (Fig. 1B). This might have led to even stronger depletion of TI-Tregs.

In addition, our data comparing therapeutic activity in the mouse tumor models clearly demonstrate the superior activity of anti-TIGIT mAbs with isotypes that exhibit higher affinity for activator FcγR that correlates with Treg specific depletion and increased intratumor CD8:Treg ratio. Our data, in disagreement with Johnston et al (3) that had reported no single agent efficacy, confirm other findings showing strong therapeutic efficacy of anti-TIGIT mAbs with an ADCC-enabled isotype (39,40). Accordingly, during the course of Etigilimab development, an anti-TIGIT mAb under clinical evaluation, it was demonstrated that preferred Treg depletion is correlated with improved antitumor therapeutic activity of isotypes engaging activatory FcγR, and peripheral Treg depletion was observed in patients during phase 1 trial (41) . Treg depletion may be explained by the better affinity of the surrogate anti-TIGIT mAb used in our study as compared to clone 10A7 (3,40). Overall, these results demonstrate the better clinical potential of anti-TIGIT mAbs with high affinity for activatory FcγR over FcγR-disabled isotypes while limiting the possible depletion of effector T cell populations.

To further understand the TIGIT expression in cancer, we compared several gene expression databases for TIGIT expression in different cancer and found the highest level of TIGIT in heme malignancies, particularly in T cell lymphoma. To understand if this observation could be linked to strong TIGIT expression in TILs or direct expression in cancer cells, we examined the presence of TIGIT in samples from patients with SS. As expected, we observed moderate TIGIT expression on the membrane of non-malignant T cells, but, more surprisingly, we also confirmed the presence of TIGIT on nearly all malignant cells in most patients. While strong TIGIT expression had been reported in $CD4^+$ T cell populations in SS samples (5), there was no distinction made between normal or malignant cells. In this case, we demonstrated, for the first time, that TIGIT can also be expressed on malignant cells. Taking advantage of this observation, we tested the potential of EOS884448 for direct cytotoxicity of tumor cells as demonstrated for molecules such as Rituximab and Trastuzumab (42,43), in samples from SS patients. The results demonstrated a clear cytotoxic potential of EOS884448 against TIGIT-expressing $CD4^+$ tumor cells, while normal $CD4^+$ T cells and NK cells were not, or only mildly, affected. We also tested this hypothesis *in vivo* in mice using tumor cells expressing mTIGIT, and showed that anti-TIGIT Ab had strong therapeutic efficacy that directly depended on antibody isotype and TIGIT expression by tumor cells. These results reveal a novel mechanism of action for anti-TIGIT Abs with direct cytotoxic potential against tumor cells in indications where TIGIT is expressed. This represents an additional previously unheralded opportunity for anti-TIGIT agents in blood cancers, which should be further explored.

Our data reveal new perspectives for the use of anti-TIGIT Abs in the clinic. In addition to their previously described mechanism of action as ICI and their ability to prevent ligand binding and negative signaling through TIGIT, while favoring engagement of co-stimulatory CD226 molecule (12), we observed additional immune-modulator functions linked to activation of other T cell subtypes and to direct cytotoxic capacity. Anti-TIGIT mAbs, when developed on ADCC enabling isotype, act by inducing 1) reversion of NK and T cell (including γδ T cells) dysfunction linked with cancer progression, 2) preferential depletion of intratumoral Treg expressing high level of TIGIT, and 3) direct cytotoxic activity of tumor

cells in specific heme malignancies. Several phase 1 and 2 trials are currently testing anti-TIGIT mAbs with different isotypes (21). Monitoring of differential efficacy between ADCC-enabled or disabled molecules should confirm whether our findings are relevant in the clinical setting. Clinical development for this class of drug should take advantage of all possible immune modulatory functions of anti-TIGIT mAbs.

Acknowledgments

Medical writing assistance was provided by John Bean PhD, Bean Medical Writing, Halle, Belgium.

References (50 max)

1. Yu X, Harden K, Gonzalez LC, Francesco M, Chiang E, Irving B, et al. The surface protein TIGIT suppresses T cell activation by promoting the generation of mature immunoregulatory dendritic cells. Nat Immunol. 2009;10:48–57.

2. Joller N, Lozano E, Burkett PR, Patel B, Xiao S, Zhu C, et al. Treg cells expressing the coinhibitory molecule TIGIT selectively inhibit proinflammatory Th1 and Th17 cell responses. Immunity. 2014;40:569–81.

3. Johnston RJ, Comps-Agrar L, Hackney J, Yu X, Huseni M, Yang Y, et al. The immunoreceptor TIGIT regulates antitumor and antiviral CD8(+) T cell effector function. Cancer Cell. 2014;26:923–37.

4. Zheng C, Zheng L, Yoo J-K, Guo H, Zhang Y, Guo X, et al. Landscape of infiltrating T cells in liver cancer revealed by single-cell sequencing. Cell. 2017;169:1342-1356.e16.

5. Jariwala N, Benoit B, Kossenkov AV, Oetjen LK, Whelan TM, Cornejo CM, et al. TIGIT and Helios are highly expressed on CD4+ T cells in Sézary syndrome patients. J Invest Dermatol. 2017;137:257–60.

6. Chew GM, Fujita T, Webb GM, Burwitz BJ, Wu HL, Reed JS, et al. TIGIT marks exhausted T cells, correlates with disease progression, and serves as a target for immune restoration in HIV and SIV Infection. PLoS Pathog. 2016;12:e1005349.

7. Fuhrman CA, Yeh W-I, Seay HR, Saikumar Lakshmi P, Chopra G, Zhang L, et al. Divergent phenotypes of human regulatory T cells expressing the receptors TIGIT and CD226. J Immunol. 2015;195:145–55.

8. Kurtulus S, Sakuishi K, Ngiow S-F, Joller N, Tan DJ, Teng MWL, et al. TIGIT predominantly regulates the immune response via regulatory T cells. J Clin Invest. 2015;125:4053–62.

9. Levin SD, Taft DW, Brandt CS, Bucher C, Howard ED, Chadwick EM, et al. Vstm3 is a member of the CD28 family and an important modulator of T-cell function. Eur J Immunol. 2011;41:902–15.

10. Lozano E, Dominguez-Villar M, Kuchroo V, Hafler DA. The TIGIT/CD226 axis regulates human T cell function. J Immunol. 2012;188:3869–75.

11. Pauken KE, Wherry EJ. TIGIT and CD226: tipping the balance between costimulatory and coinhibitory molecules to augment the cancer immunotherapy toolkit. Cancer Cell. 2014;26:785–7.

12. Manieri NA, Chiang EY, Grogan JL. TIGIT: a key inhibitor of the cancer immunity Cycle. Trends Immunol. 2017;38:20–8.

13. Li X, Wang R, Fan P, Yao X, Qin L, Peng Y, et al. A comprehensive analysis of key immune checkpoint receptors on tumor-infiltrating T cells from multiple types of cancer. Front Oncol. 2019;9:1066.

14. Solomon BL, Garrido-Laguna I. TIGIT: a novel immunotherapy target moving from bench to bedside. Cancer Immunol Immunother. 2018;67:1659–67.

15. Zhang Q, Bi J, Zheng X, Chen Y, Wang H, Wu W, et al. Blockade of the checkpoint receptor TIGIT prevents NK cell exhaustion and elicits potent anti-tumor immunity. Nat Immunol. 2018;19:723–32.

16. Hung AL, Maxwell R, Theodros D, Belcaid Z, Mathios D, Luksik AS, et al. TIGIT and PD-1 dual checkpoint blockade enhances antitumor immunity and survival in GBM. Oncoimmunology. 2018;7:e1466769.

17. Guillerey C, Harjunpää H, Carrié N, Kassem S, Teo T, Miles K, et al. TIGIT immune checkpoint blockade restores CD8+ T-cell immunity against multiple myeloma. Blood. 2018;132:1689–94.

18. Dixon KO, Schorer M, Nevin J, Etminan Y, Amoozgar Z, Kondo T, et al. Functional Anti-tIGIT antibodies regulate development of autoimmunity and antitumor immunity. J Immunol. 2018;200:3000–7.

19. Minnie SA, Kuns RD, Gartlan KH, Zhang P, Wilkinson AN, Samson L, et al. Myeloma escape after stem cell transplantation is a consequence of T-cell exhaustion and is prevented by TIGIT blockade. Blood. 2018;132:1675–88.

20. Chauvin J-M, Pagliano O, Fourcade J, Sun Z, Wang H, Sander C, et al. TIGIT and PD-1 impair tumor antigen-specific $CD8^+$ T cells in melanoma patients. J Clin Invest. 2015;125:2046–58.

21. Sanchez-Correa B, Valhondo I, Hassouneh F, Lopez-Sejas N, Pera A, Bergua JM, et al. DNAM-1 and the TIGIT/PVRIG/TACTILE axis: novel immune checkpoints for natural killer cell-based cancer immunotherapy. Cancers [Internet]. 2019 [cited 2019 Dec 12];11:877. Available from: https://www.mdpi.com/2072-6694/11/6/877

22. Gomes B, Driessens G, Bartlett D, Cai D, Cauwenberghs S, Crosignani S, et al. Characterization of the selective indoleamine 2,3-dioxygenase-1 (IDO1) catalytic inhibitor EOS200271/PF-06840003 supports IDO1 as a critical resistance mechanism to PD-(L)1 blockade therapy. Mol Cancer Ther [Internet]. 2018 [cited 2019 Dec 13];17:2530–42. Available from: http://mct.aacrjournals.org/lookup/doi/10.1158/1535-7163.MCT-17-1104

23. Beers SA, French RR, Chan HT, Lim SH, Jarrett TC, Vidal RM,et al. Antigenic modulation limits the efficacy of anti-CD20 antibodies: implications for antibody selection.. Blood. 2010;115(25):5191-201. doi: 10.1182/blood-2010-01-263533.

24. Marie-Cardine A, Viaud N, Thonnart N, Joly R, Chanteux S, Gauthier L, et al. IPH4102, a humanized KIR3DL2 antibody with potent activity against cutaneous T-cell lymphoma. Cancer Res. 2014;74:6060–70.

25. Liu C, Cripe TP, Kim M-O. Statistical issues in longitudinal data analysis for treatment efficacy studies in the biomedical sciences. Mol Ther. 2010;18:1724–30.

26. Couzi L, Pitard V, Moreau J-F, Merville P, Déchanet-Merville J. Direct and indirect effects of cytomegalovirus-induced γδ T cells after kidney transplantation. Front Immunol [Internet]. 2015 [cited 2019 Dec 19];6. Available from: https://www.frontiersin.org/articles/10.3389/fimmu.2015.00003/full

27. Seidel JA, Otsuka A, Kabashima K. Anti-PD-1 and anti-CTLA-4 therapies in cancer: mechanisms of action, efficacy, and limitations. Front Oncol. 2018;8:86.

28. Restifo NP, Smyth MJ, Snyder A. Acquired resistance to immunotherapy and future challenges. Nat Rev Cancer. 2016;16:121–6.

29. Gentles AJ, Newman AM, Liu CL, Bratman SV, Feng W, Kim D, et al. The prognostic landscape of genes and infiltrating immune cells across human cancers. Nat Med. 2015;21:938–45.

30. Meraviglia S, Lo Presti E, Tosolini M, La Mendola C, Orlando V, Todaro M, et al. Distinctive features of tumor-infiltrating γδ T lymphocytes in human colorectal cancer. Oncoimmunology. 2017;6:e1347742.

31. Zumwalde NA, Sharma A, Xu X, Ma S, Schneider CL, Romero-Masters JC, et al. Adoptively transferred V**γ**9V**δ**2 T cells show potent antitumor effects in a preclinical B cell lymphomagenesis model. JCI Insight [Internet]. 2017 [cited 2019 Dec 12];2. Available from: https://insight.jci.org/articles/view/93179

32. Lo Presti E, Pizzolato G, Corsale AM, Caccamo N, Sireci G, Dieli F, et al. γδ T cells and tumor microenvironment: from immunosurveillance to tumor evasion. Front Immunol [Internet]. 2018 [cited 2019 Dec 12];9. Available from: https://www.ncbi.nlm.nih.gov/pmc/articles/PMC6013569/

33. Silva-Santos B, Serre K, Norell H. γδ T cells in cancer. Nat Rev Immunol [Internet]. 2015 [cited 2019 Dec 19];15:683–91. Available from: https://www.nature.com/articles/nri3904

34. Kim HR, Park HJ, Son J, Lee JG, Chung KY, Cho NH, et al. Tumor microenvironment dictates regulatory T cell phenotype: upregulated immune checkpoints reinforce suppressive function. Journal for ImmunoTherapy of Cancer [Internet]. 2019 [cited 2019 Dec 12];7:339. Available from: https://doi.org/10.1186/s40425-019-0785-8

35. Shang B, Liu Y, Jiang S, Liu Y. Prognostic value of tumor-infiltrating FoxP3+ regulatory T cells in cancers: a systematic review and meta-analysis. Sci Rep. 2015;5:15179.

36. Schoenhals JE, Cushman TR, Barsoumian HB, Li A, Cadena AP, Niknam S, et al. Anti-glucocorticoid-induced tumor necrosis factor–related protein (GITR) therapy overcomes radiation-induced Treg immunosuppression and drives abscopal effects. Front Immunol [Internet]. 2018 [cited 2019 Dec 12];9. Available from: https://www.ncbi.nlm.nih.gov/pmc/articles/PMC6158365/

37. Arce Vargas F, Furness AJS, Litchfield K, Joshi K, Rosenthal R, Ghorani E, et al. Fc effector function contributes to the activity of human anti-CTLA-4 antibodies. Cancer Cell. 2018;33:649-663.e4.

38. Buchan SL, Dou L, Remer M, Booth SG, Dunn SN, Lai C, et al. Antibodies to Costimulatory Receptor 4-1BB Enhance Anti-tumor Immunity via T Regulatory Cell Depletion and Promotion of CD8 T Cell Effector Function. Immunity 2018;49(5):958-970.

39. Argast GM, Cancilla B, Cattaruzza F, Yeung P, Scolan E le, Harris R, et al. Abstract 5627: Anti-TIGIT biomarker study: inhibition of TIGIT induces loss of Tregs from tumors and requires effector function for tumor growth inhibition. Cancer Res [Internet]. 2018 [cited 2019 Dec 12];78:5627–5627. Available from: https://cancerres.aacrjournals.org/content/78/13_Supplement/5627

40. Waight JD, Chand D, Dietrich S, Gombos R, Horn T, Gonzalez AM, et al. Selective FcγR co-engagement on APCs modulates the activity of therapeutic antibodies targeting T cell antigens. Cancer Cell. 2018;33:1033-1047.e5.

41. Sharma S, Moore KN, Mettu NB, Garrido-Laguna I, Ulahannan SV, Khemka V, et al. Poster 289 : Initial results from a phase 1a/b study of etigilimab (OMP-313M32), an anti-T cell immunoreceptor with Ig and ITIM domains (TIGIT) antibody, in advanced solid tumors.J. Immunotherapy Cancer 2018 ; **6(Suppl1) :**114 :147-47 . Available from : https://jitc.biomedcentral.com/track/pdf/10.1186/s40425-018-0422-y

42. Hudis CA. Trastuzumab--mechanism of action and use in clinical practice. N Engl J Med. 2007;357:39–51.

43. Salles G, Barrett M, Foà R, Maurer J, O'Brien S, Valente N, et al. Rituximab in B-cell hematologic malignancies: a review of 20 years of clinical experience. Adv Ther. 2017;34:2232–73.

Figures legends

Figure 1. CD155 and TIGIT are highly expressed in various solid cancers. A) (Left panel): Representative IHC picture of CD155 expression by tumor cells in a kidney cancer sample. Proportion of $CD155^{high}$ cells were analyzed within tumor area ($pancytokeratin^{+}$) by automated quantification (Visiopharm® software) of IHC-stained tissue microarrays (n=284 samples from 10 different indications). B and C) PBMCs from healthy donors (n=10) matched PBMCs and dissociated tumor samples from different cancer indications (n=12) were analyzed by Flow Cytometry for the frequency of TIGIT expressing cells on different immune subsets (B) or for the number of TIGIT receptor expressed at the membrane (C). Data are represented as Tukey plots. *p < 0.05; **p < 0.001; **p < 0.0001 by Two-Way Anova analysis with multiple comparisons, using GraphPad Prism.

Figure 2. TIGIT-expressing TILs are not functional, but T cell activity can be restored by antagonist anti-TIGIT Ab. (A) FACS analysis of a representative sample ccRCC (clear cell renal cell carcinoma). The dissociated sample were stimulated 3h with a mix of PMA/ionomycin in presence of Monensin and Brefeldin A. Data represent multiple expression (Boolean gate) of the frequency for IFNγ, IL-2 or TNFα inside the ($TIGIT^{+}$ or $TIGIT^{-}$) $CD4^{+}$ and $CD8^{+}$ TILs. **(B)** FACS analyses of $CD4^{+}$ and $CD8^{+}$ T lymphocytes in blood cancer samples (n=3 : 1 Lung, 1 Melanoma and 1 RCC) and tumor primary cancer samples (n=5 : 2 Breast, 1 Lung, 1 Melanoma and 1 RCC) for production of TNFα or IFNγ after stimulation (as in Fig1A). Data represent expression by frequency of IFNγ and TNFα inside the $TIGIT^{+}$ T cells $CD4^{+}$ and $CD8^{+}$ TILs. Data are represented as Tukey plot *****p < 0.05; **p < 0.01 by Student's t-test. **(C)** Dose-response curve of the capacity of anti-TIGIT EOS884448 Ab to induce IFNγ release by $CD8^{+}$ T cells from healthy donor PBMCS activated in the presence of CD155-expressing cells. Data are presented as mean of IFNγ concentration in supernatant (+/- SD). This graph shows one representative experiment out of eight.

Figure 3. TIGIT is expressed on γδ T cells and has suppressive activity. A-B) Immune populations from CMV-seropositive and negative human volunteers were tested by flow cytometry for TIGIT (A) or PD1 (B) expression (n=22). (C-D) $V\delta2^{-}$ T cells were isolated and stimulated *in vitro* by anti-Vδ1 in the presence or absence of CD155 and/or anti-TIGIT Ab EOS884448. Secreted IFNγ (C) or other pro-inflammatory cytokines (D) were measured by ELISA (n=5 donors). Data represent dot plot (A-B) with mean and standard deviation or Tukey plot (C-D). *p < 0.05; **p < 0.01 by Student's t-test.

Figure 4. EOS884448 triggers preferential ADCC of Tregs *in vitro*.
A) % of specific lysis analyzed on gated $CD45RO^{+}CD4^{+}$ and $CD45RO^{+}CD8^{+}$ T cells, Tregs, and $CD19^{+}$ cells by FACS analysis in PBMCs isolated from a lung cancer patient blood sample incubated *ex vivo* with either EOS884448, isotype control, or Rituximab. Results are shown as mean +/-SEM from triplicates. B) Dot plot graph showing the mean % of specific lysis analyzed as in A) on PBMCs from several solid cancer indications including bladder (n=1) (light grey square), breast (n=2) (dark grey square) , colon (n=3) (black triangle), and lung (n=1) (black hexagon) Cancer. The analyzed populations corresponding to the same donor are matched with a line. Results are expressed as mean value of triplicates for each population. C) Graph showing pooled data analysis on the number of TIGIT molecules per cell in populations from different cancer patients analyzed in B). *p < 0.05; **p < 0.01 versus % of specific lysis in Treg by Student's t-test.

Figure 5: Anti-TIGIT mIgG2a antibody shows strong anti-tumor activity *in vivo*. (A) Median tumor growth curves for mice treated with mIgG2a isotype control or anti-TIGIT mIgG2a in CT26 colon carcinoma or Hepa1-6 hepatocarcinoma mouse models (n=10 mice/group); graph is representative of 3 independent experiments. (B-C) Median tumor growth curves for mice treated with mIgG2a isotype, anti-TIGIT mIgG2a, or anti-TIGIT mIgG1 in CT26 tumor bearing wild type (B) or FcR γ chain KO (C) mice; results shown in C are representative of two independent experiments. (D) Percent change in Treg population and $CD8^+$ T cell population in CT26 dissociated tumors after *in vivo* treatment with anti-TIGIT mIgG2a, anti-TIGIT mIgG1 or mIgG2a isotype controls. Data are represented as a Tukey plot normalized to the average of isotype treated animals (n=8/group) and are representative of 3 independent experiments. (E) Percent change in IFNγ-producing cells among CD4 and CD8 T cell populations in CT26 dissociated tumors after *in vivo* treatment with anti-TIGIT mIgG2a, anti-TIGIT mIgG1, or mIgG2a isotype control and *ex vivo* stimulation with PMA/ionomycin. Data are represented as a Tukey plots normalized to the average of isotype treated animals (n=8/group) and are representative of 3 independent experiments. (F) Median tumor growth curves for mice treated with PBS, anti-TIGIT mIgG2a, or ICI indicated in the legend, as single agent or combined with anti-TIGIT (n=10 mice/group); same combination activity was observed in PanO2 and MC38 tumor models. Linear mixed model was used for statistical analysis of tumor growth curves; Student's t-test was used for analysis of Tukey plots; *$p < 0.05$; **$p < 0.01$; ***$p<0.001$ versus isotype or PBS treated group.

Figure 6: TIGIT is expressed on tumor cells and represents a target for ADCC. (A) Flow cytometry showing gating strategy and TIGIT expression on malignant ($TCRVb^+$ $CD3^+$ $CD4^+$) and non-malignant ($TCRVb^-$ $CD3^+$ $CD4^+$) cells. (B) Dot plots and median percentage of $TIGIT^+$ cells among malignant versus non-malignant $CD4^+$ T cells (n=23 patients). (C) Cell death monitored through the incorporation of 7-AAD of the malignant CD4 T cells, non-malignant CD4 T cells and NK cells in presence of isotype control or anti-TIGIT Ab EOS884448. Results are shown for one representative donor out of four and are expressed as the % of $7\text{-}AAD^+$ cells among each population at a given E:T ratio. (D) Median tumor growth curves for EL4-mTIGIT (left panel) and EL4-GFP (right panel) tumors treated with hIgG1 isotype, anti-TIGIT hIgG1 or anti-TIGIT hIgG1-N297A (n=10 mice/group). ***$p<0.001$ versus isotype treated group.

Figure 1

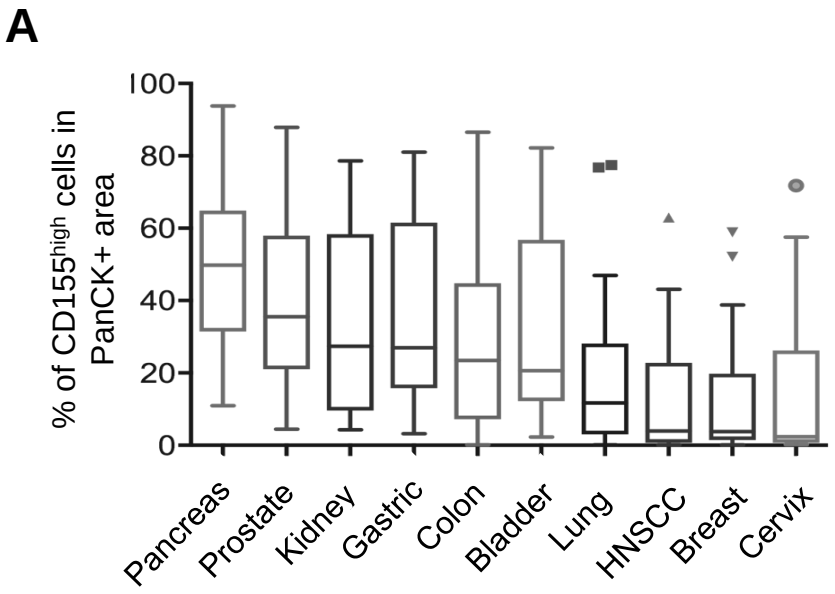
A
% of CD155high cells in PanCK+ area
100
80
60
40
20
0
Pancreas
Prostate
Kidney
Gastric
Colon
Bladder
Lung
HNSCC
Breast
Cervix

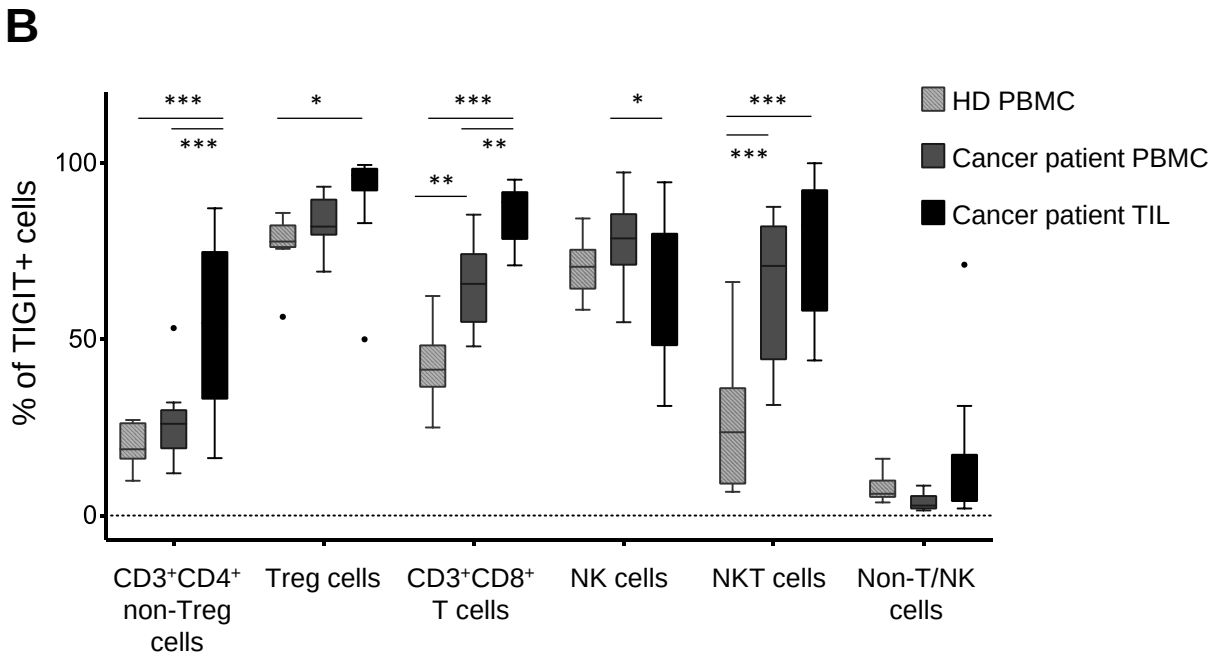
B
% of TIGIT+ cells
100
50
0
***
***
*
***
**
**
*
***
***
HD PBMC
Cancer patient PBMC
Cancer patient TIL
CD3+CD4+ non-Treg cells
Treg cells
CD3+CD8+ T cells
NK cells
NKT cells
Non-T/NK cells

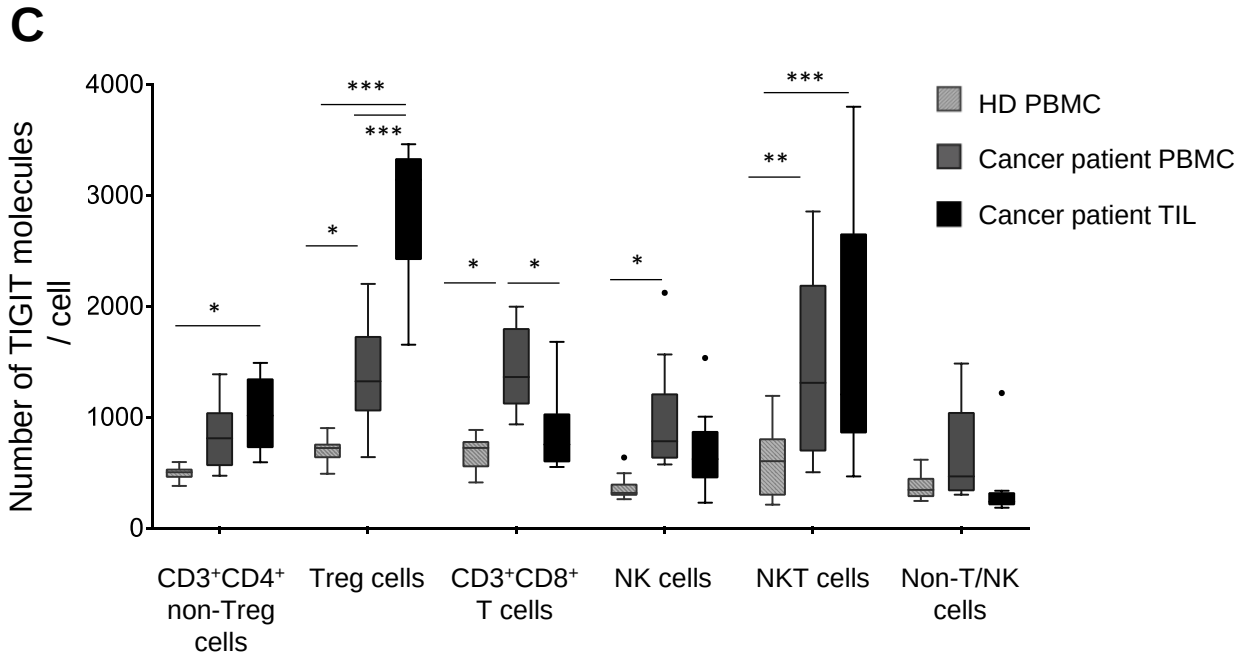
C
Number of TIGIT molecules / cell
4000
3000
2000
1000
0
*
***
***
*
*
*
*
***
**
HD PBMC
Cancer patient PBMC
Cancer patient TIL
CD3+CD4+ non-Treg cells
Treg cells
CD3+CD8+ T cells
NK cells
NKT cells
Non-T/NK cells

Figure 2

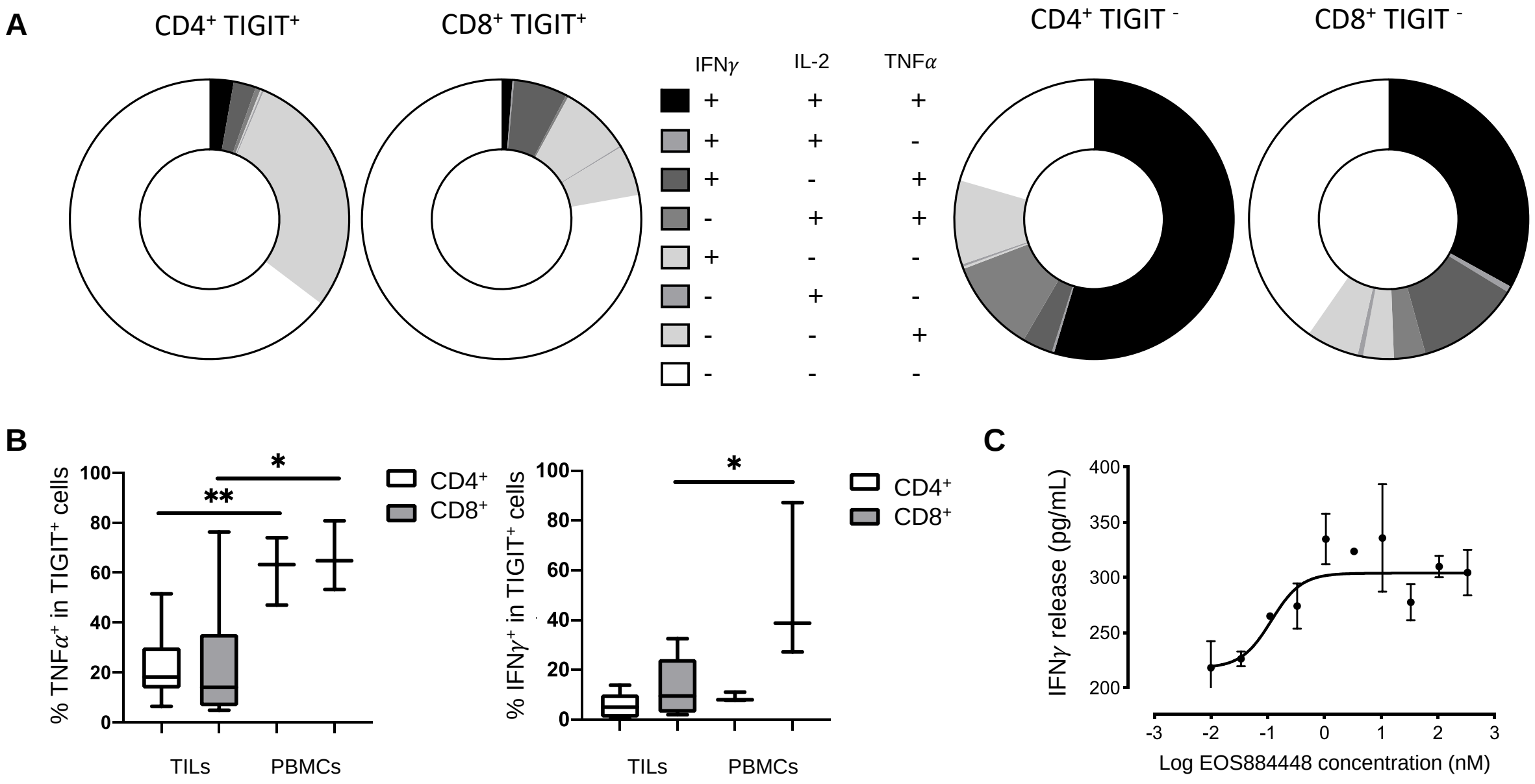
A
CD4+ TIGIT+
CD8+ TIGIT+
IFNγ
IL-2
TNFα
CD4+ TIGIT -
CD8+ TIGIT -
B
% TNFα+ in TIGIT+ cells
% IFNγ+ in TIGIT+ cells
CD4+
CD8+
TILs
PBMCs
C
IFNγ release (pg/mL)
Log EOS884448 concentration (nM)

Figure 3

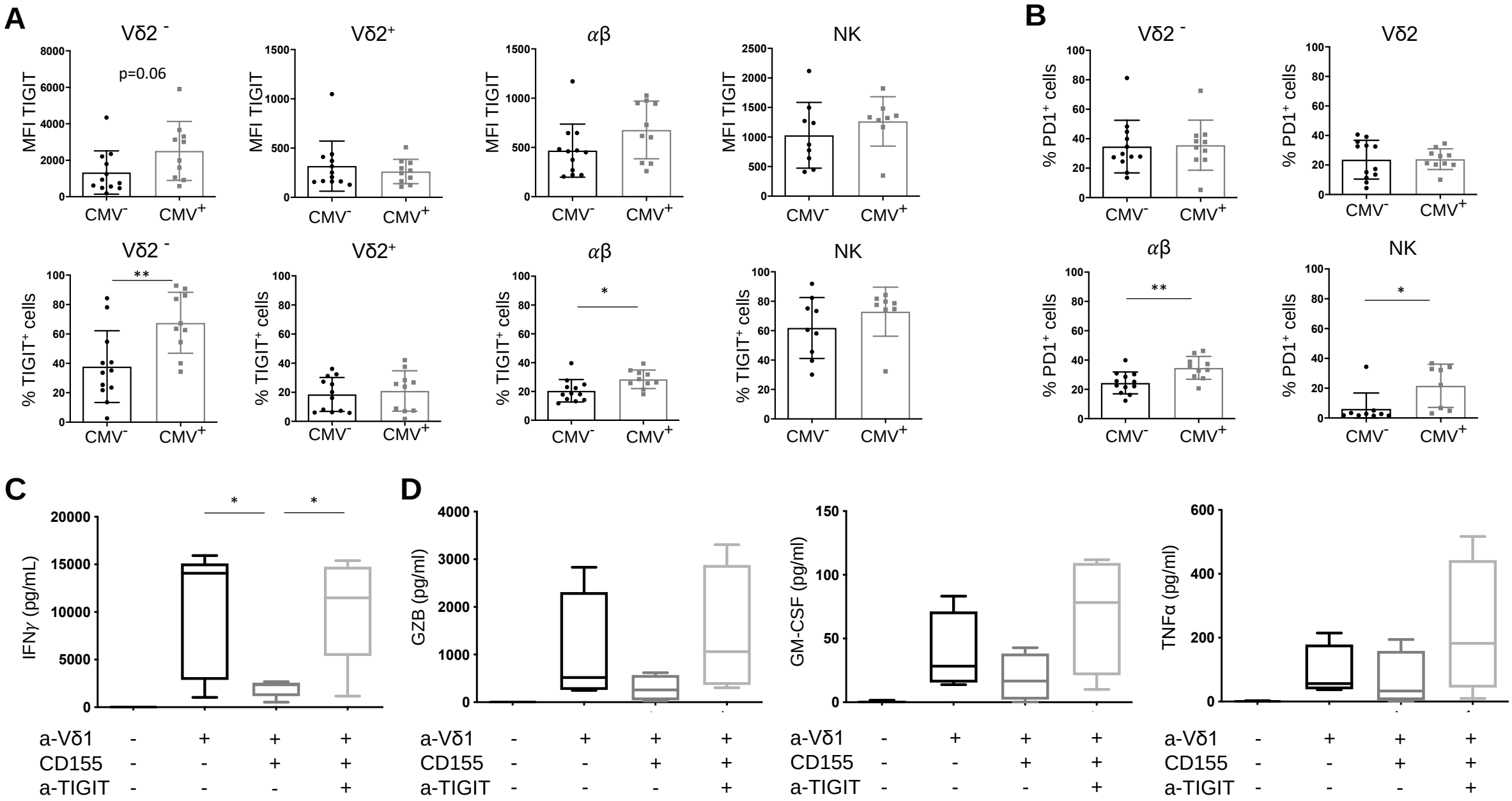
A
Vδ2 -
Vδ2+
αβ
NK
MFI TIGIT
p=0.06
% TIGIT+ cells
**
*
CMV-
CMV+
B
% PD1+ cells
C
IFNγ (pg/mL)
D
GZB (pg/ml)
GM-CSF (pg/ml)
TNFα (pg/ml)
a-Vδ1
CD155
a-TIGIT

Figure 4

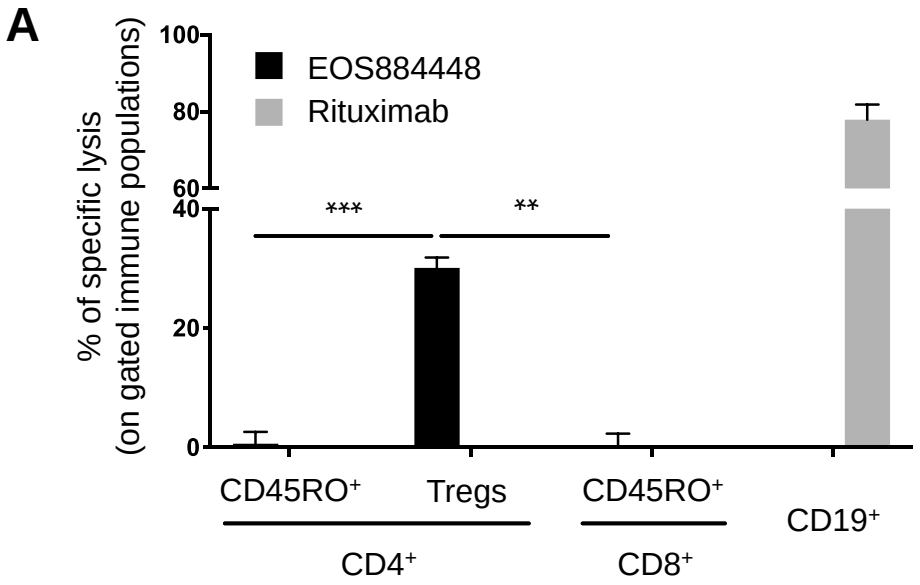
A
EOS884448
Rituximab
% of specific lysis
(on gated immune populations)
100
80
60
40
20
0
***
**
CD45RO+
Tregs
CD45RO+
CD19+
CD4+
CD8+

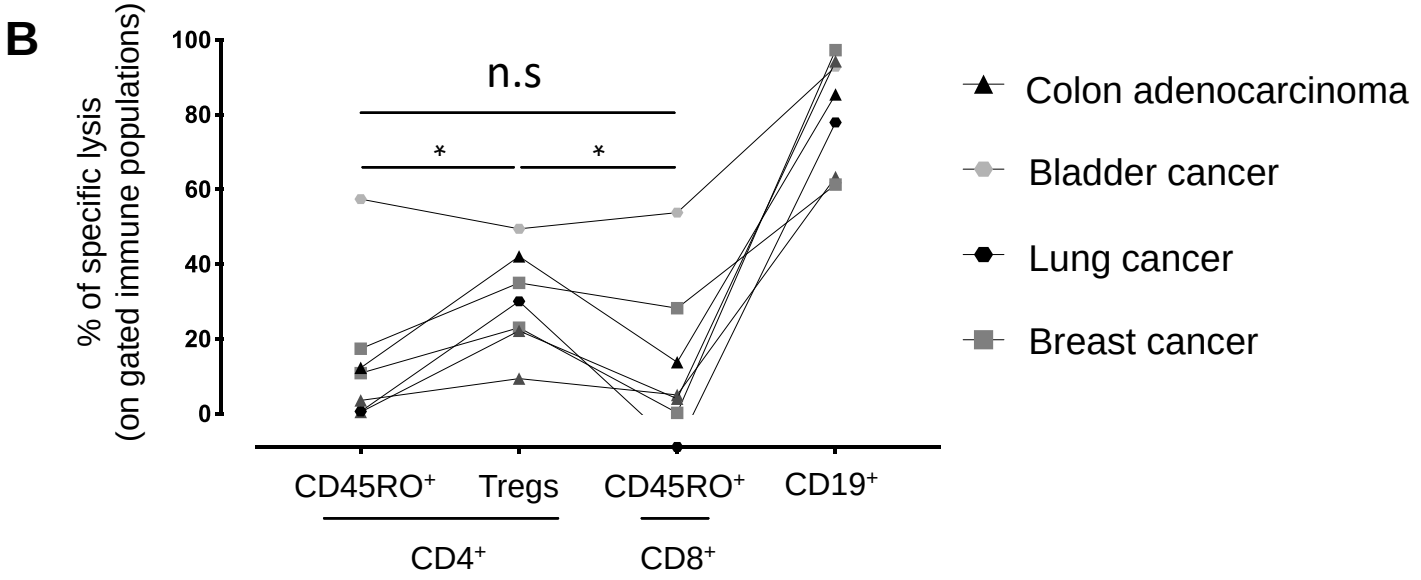
B
% of specific lysis
(on gated immune populations)
100
80
60
40
20
0
n.s
*
*
CD45RO+
Tregs
CD45RO+
CD19+
CD4+
CD8+
Colon adenocarcinoma
Bladder cancer
Lung cancer
Breast cancer

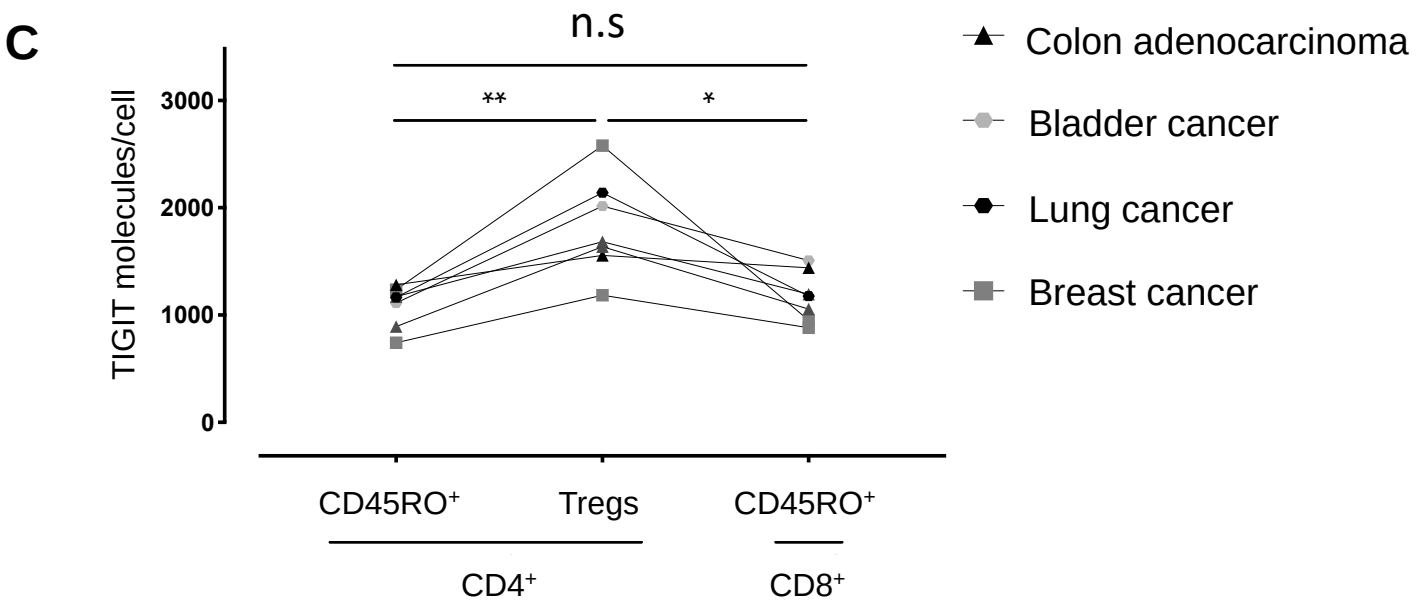
C
TIGIT molecules/cell
3000
2000
1000
0
n.s
**
*
CD45RO+
Tregs
CD45RO+
CD4+
CD8+
Colon adenocarcinoma
Bladder cancer
Lung cancer
Breast cancer

Figure 5

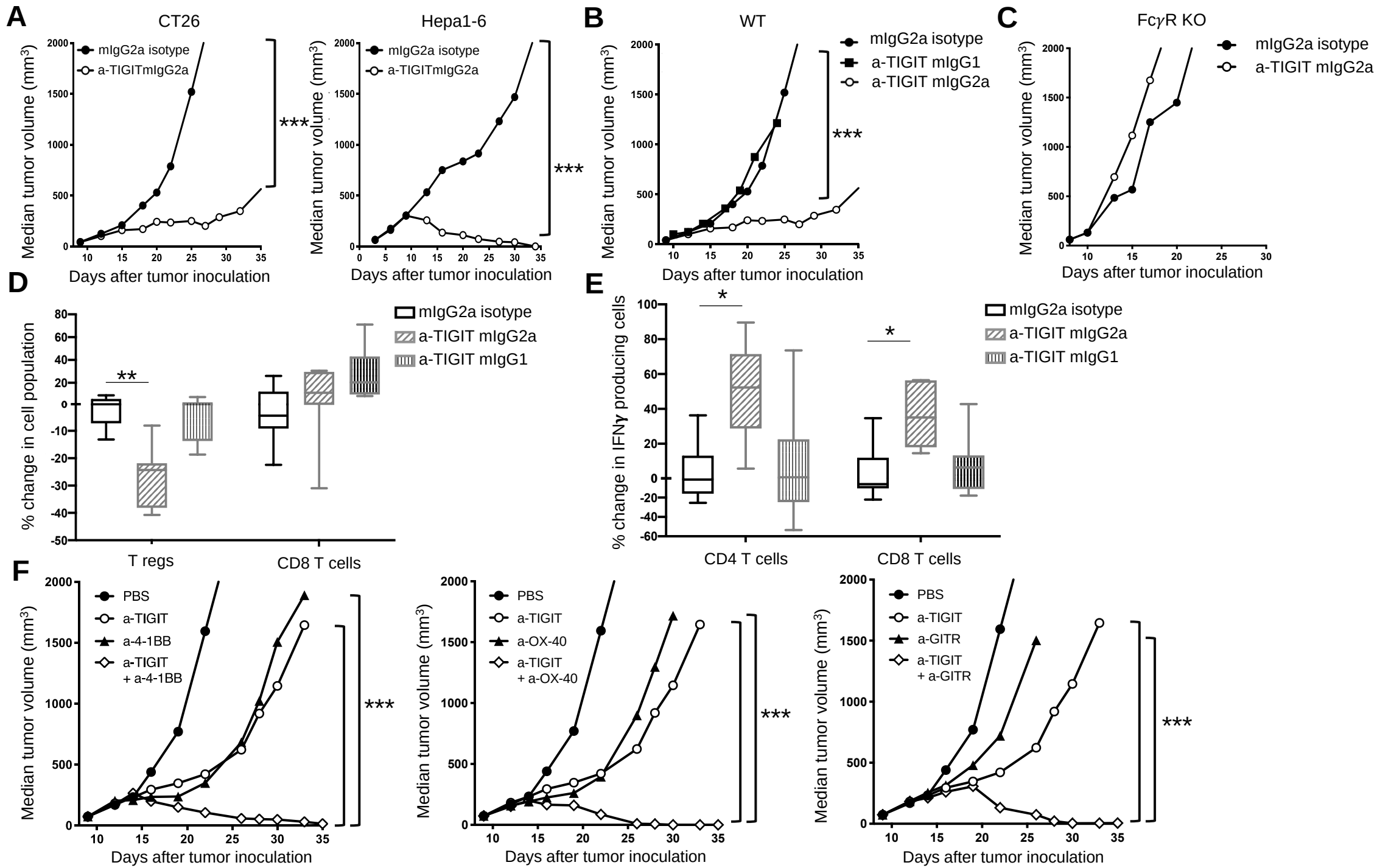
A
CT26
Hepa1-6
mIgG2a isotype
a-TIGITmIgG2a
Median tumor volume (mm3)
Days after tumor inoculation
***
B
WT
mIgG2a isotype
a-TIGIT mIgG1
a-TIGIT mIgG2a
C
FcγR KO
D
% change in cell population
T regs
CD8 T cells
**
E
% change in IFNγ producing cells
CD4 T cells
CD8 T cells
*
F
PBS
a-TIGIT
a-4-1BB
a-TIGIT
+ a-4-1BB
a-OX-40
+ a-OX-40
a-GITR
+ a-GITR

Figure 6

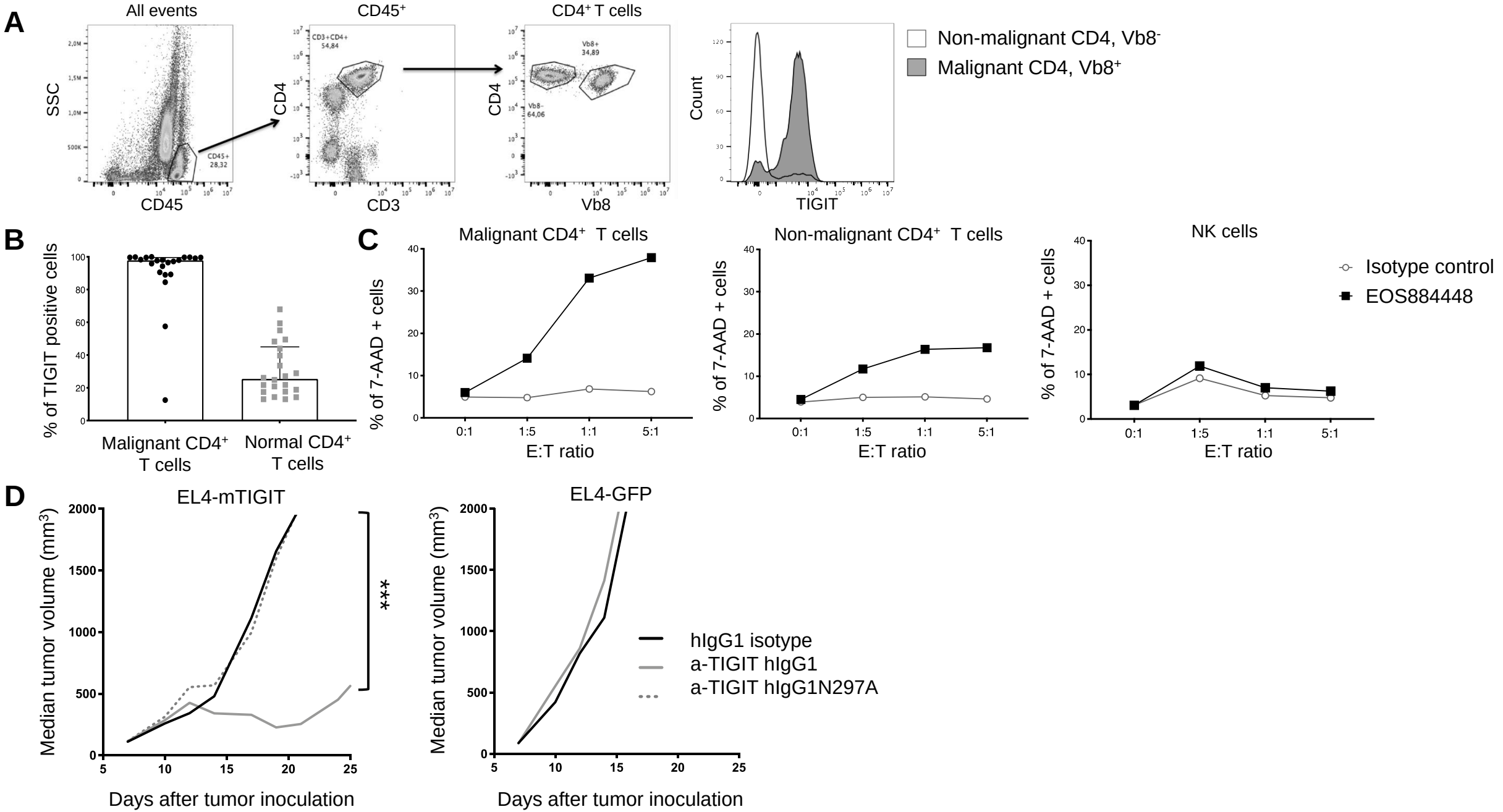
A
All events
CD45+
CD4+ T cells
SSC
CD45
CD4
CD3
Vb8
Count
TIGIT
Non-malignant CD4, Vb8-
Malignant CD4, Vb8+
B
% of TIGIT positive cells
Malignant CD4+ T cells
Normal CD4+ T cells
C
Malignant CD4+ T cells
Non-malignant CD4+ T cells
NK cells
% of 7-AAD + cells
E:T ratio
Isotype control
EOS884448
D
EL4-mTIGIT
EL4-GFP
Median tumor volume (mm3)
Days after tumor inoculation
***
hIgG1 isotype
a-TIGIT hIgG1
a-TIGIT hIgG1N297A